Flight-Test Evaluation of Landing Gear Noise Reduction Technologies

Mehdi R. Khorrami,[1] David P. Lockard,[2] William M. Humphreys, Jr.[3]
NASA Langley Research Center, Hampton, VA, 23681, USA

and
Patricio A. Ravetta[4]
AVEC Inc., Blacksburg, Virginia 24060, USA

Results from the third Acoustics Research Measurements flight test, conducted under the NASA Flight Demonstrations and Capabilities project, are presented and discussed. The test evaluated landing gear and gear cavity noise mitigation technologies installed on a NASA Gulfstream G-III. Aircraft configurations with and without main landing gear treatments were flown at several flap deflections to determine the acoustic performance of the technologies for aircraft equipped with conventional Fowler flaps. With the aircraft flying an approach path and engines at "ground-idle," extensive acoustic measurements were acquired with a phased microphone array system. Computed beamform maps were used to examine the effectiveness of the tested technologies in reducing the strength of the noise sources generated by the main landing gear. Various integration regions were devised to extract the farfield noise spectra associated with the treated and untreated landing gear configurations. Analyses of the gathered acoustic data demonstrate that significant noise reduction was achieved. However, the full noise reduction potential of the technologies could not be determined because of contamination from flap inboard edge noise and other secondary sources.

Nomenclature

AOA	=	Angle of attack
f	=	Frequency
ACTE	=	Adaptive Compliant Trailing Edge
AFB	=	Air Force Base
AFRC	=	Armstrong Flight Research Center
AFRL	=	U. S. Air Force Research Laboratory
ARMD	=	Aeronautics Research Mission Directorate
EPNL	=	Effective Perceived Noise Level
ERA	=	Environmentally Responsible Aviation
FDC	=	Flight Demonstrations and Capabilities
MLG	=	Main landing gear
NR	=	Noise reduction
PKF	=	Porous knee fairing
PSD	=	Power spectral density
SCRAT	=	SubsoniC Research Aircraft Testbed
SPL	=	Sound pressure level
UF	=	Upper fairings

---

[1] Aerospace Engineer, Computational AeroSciences Branch, Associate Fellow AIAA.
[2] Aerospace Engineer, Computational AeroSciences Branch, Senior Member AIAA.
[3] Aerospace Engineer, Advanced Measurement and Data Systems Branch, Associate Fellow AIAA.
[4] Co-owner, Chief Research Engineer, Senior Member AIAA.

I. Introduction

The availability of a broad range of technologies with superior aeroacoustic performance is essential for the production of quiet, efficient aircraft that will foster continued growth [1, 2] in international civil aviation while reducing community noise. Noise generated by the airframe dominates the acoustic spectrum of most modern aircraft during landing, with the undercarriage and wing high-lift devices, such as flaps and slats, constituting the primary sources [3].

Development and maturation of viable technologies that substantially reduce the airframe component of aircraft noise is of importance to the NASA Aeronautics Research Mission Directorate (ARMD). A major effort on airframe noise reduction was initiated under the Environmentally Responsible Aviation (ERA) project. Numerous concepts for mitigating the noise produced by aircraft flaps and undercarriage were conceived and evaluated via extensive model-scale testing and high-fidelity simulations [4]. After the ERA project ended in 2015, a full-scale evaluation of the most promising technologies in a relevant environment was pursued under the Flight Demonstrations and Capabilities (FDC) project. The Acoustics Research Measurements (ARM) flights, a campaign that comprised three separate two-and-a-half-month long tests, were completed over a two-year period between 2016 and 2018. Select landing gear and flap noise reduction (NR) technologies were integrated onto a NASA Gulfstream G-III aircraft to determine their individual and aggregated effectiveness.

The first campaign (ARM-I, 2016) evaluated the Adaptive Compliant Trailing Edge (ACTE) concept as a mechanism to reduce flap noise [5, 6]. The second test (ARM-II, 2017) assessed the effectiveness of various main landing gear (MLG) and gear cavity NR treatments in combination with the ACTE technology [5, 6]. For the third flight test (ARM-III, 2018), the ACTE flaps were removed and the original Fowler flaps were reinstalled on the G-III aircraft to obtain baseline flap and landing gear data, and to assess the noise reduction capability of the landing gear technologies for conventional flaps. Extensive acoustic measurements were acquired during the ARM tests with a NASA-developed phased microphone array comprised of 185 sensors [7]. Additionally, three pole-mounted microphones were used for Effective Perceived Noise Level (EPNL) measurements. Processed phased array data from the ARM-I and ARM-II tests, presented in Ref. [5], demonstrated that significant reductions in acoustic energy for the sources associated with the flaps and MLG were obtained when the ACTE concept and the gear treatments were installed. The effectiveness of the noise reduction technologies was observed over a wide range of forward directivity angles [5].

An in-depth analysis of the acoustic data acquired during the ARM-III test is presented in this paper. Data quality and repeatability are assessed for various baseline and treated landing gear configurations, and the acoustic performance of landing gear noise reductions technologies is evaluated for conventional (Fowler) flaps.

II. Test Aircraft and Test Site

All ARM flights were conducted with two Gulfstream G-III aircraft based at the NASA Armstrong Flight Research Center (AFRC). The primary G-III used during the ARM-I and ARM-II tests was the SubsoniC Research Aircraft Testbed (SCRAT), also known by its tail number as "804" (see Fig. 1a) [5]. The heavily instrumented 804 allows in-flight recording of aircraft parameters such as global position, angle of attack (AOA), and true airspeed (TAS). The second aircraft, also known by its tail number as "808" (Fig. 1b), was a stock G-III that served as the initial baseline configuration. For the ARM-III test, the ACTE flaps were removed from 804 and the original Fowler flaps were reinstalled. This conversion allowed 804 to serve both as the baseline, unmodified testbed and a vehicle for evaluating the acoustic performance of the MLG and cavity NR technologies in conjunction with conventional (Fowler) flaps. Detailed information for the 804 and 808 aircraft is provided in Ref. [6].

Both ARM-I and ARM-II flight tests were conducted on the Rogers dry lakebed at Edwards Air Force Base (AFB) in Southern California. The microphone array and pole-mounted certification microphones were deployed at the North end of runway 18L. This location provided ample flat terrain for the disposition of various elements of the ground operations and data collection hardware. To avoid possible delays/cancellations due to rainy spring weather, the microphone array and certification microphones were deployed on the overrun section of inactive runway 24 of North base at Edwards AFB during ARM-III. Although the new deployment site was relatively close to the lakebed site used during ARM-I and ARM-II, it introduced several notable differences that affected the acoustic measurements. Foremost among these differences were a) placement of the microphone array on a paved, concrete surface versus the compact dirt surface of the lakebed during ARM-I and ARM-II, and b) closer proximity of the inactive runway to a major highway just outside the AFB grounds that resulted in higher background noise levels.

a) NASA 804 (SCRAT)   b) NASA 808

Fig. 1 Gulfstream G-III aircraft with Fowler flaps.

A. Noise Reduction Technologies

The landing gear NR technologies evaluated during the ARM flight tests were a collection of fairings installed on the main landing gear and two cavity treatments. The G-III main landing gear with and without acoustic treatment is shown in Fig. 2. The fairings comprise the porous knee fairing (PKF) covering the front post plus an assortment of smaller fairings that are collectively referred to as upper fairings (UF). The two cavity treatments consisted of a stretchable mesh and a concept that combines chevrons at the leading edge of the cavity with an acoustic foam treatment on the downstream side of the cavity. A close-up view of these two concepts, as installed on the 804 aircraft, is shown in Fig. 3. A full description of these technologies can be found in Refs. [5, 6].
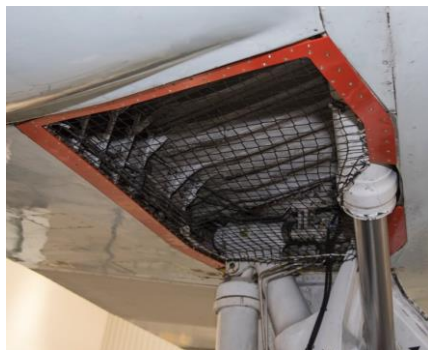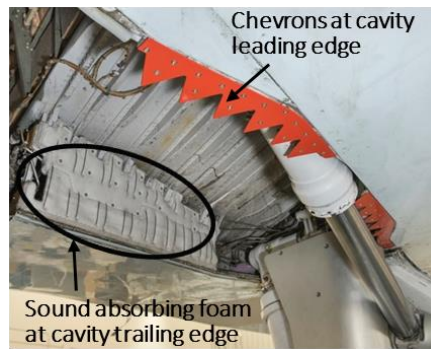

a)   Baseline   b) With fairings installed

Fig. 2 Gulfstream G-III main landing gear. Baseline gear is shown in its compressed, on the ground state; the faired gear is depicted in its stretched, in-flight state (from Ref. [5]).

a) Stretchable mesh   b) Chevrons and acoustic foam

Fig. 3 Flight tested main gear cavity treatments as installed on 804 aircraft (from Ref. [5]).

III.   Test Procedure and Measurements

A full account of the flight and ground operations in support of the airframe noise test campaign is provided in Ref. [6]. Recording of local meteorological conditions, their corresponding acoustic data corrections, and microphone array data processing techniques used in the present acoustic analyses are the same as those employed for ARM-I and ARM-II test data [5, 8]. Background noise levels at the new location were higher than those encountered during the first two tests, as noted earlier.

Adhering to the procedure established for ARM-I and ARM-II, all array flyovers were executed with the aircraft engines operating at "ground-idle" to minimize contamination of the acoustic measurements by propulsion noise. As in the previous ARM tests, to ensure that the gathered data were statistically meaningful, multiple passes during each flight and multiple flights on different days were executed for most aircraft configurations. To determine velocity scaling, acoustic measurements for most configurations of interest were obtained at 140, 150, and 165 kts with the middle value representing the speed at which the majority of the measurements were taken. With the completion of ARM-III, data collection spanned multiple years for a few, select configurations. As a result, pass-to-pass, day-to-day, and year-to-year variations in the measured noise signatures and the resulting uncertainties can be determined and assessed.

A. Array Data Processing

A description of the processing approach applied to the microphone array data collected during the ARM tests is provided in Ref. [5]. An overview highlighting the salient aspects of the methodology is provided here for completeness.

A time-domain, delay-and-sum beamformer with diagonal removal coupled with CLEAN deconvolution, both available within AVEC's Phased Array Software Suite [9], was used to process the microphone array data collected during the ARM tests. Beamform (source localization) maps were generated on a square, 100 ft by 100 ft (30.5 m by 30.5 m) planar grid covering the entire aircraft. A grid size of 201×201 points, representing a spatial resolution of 6 in. (15.25 cm), was deemed adequate for generation of the maps that provided the position and sound pressure level (SPL) of the sources. The results presented here were scaled to an altitude of 394 ft. (120 m) under the assumption of spherical spreading for pressure ($p'^2 \sim 1/r^2$).

The maps provide valuable insight into the effect that the NR technologies have on the intended noise sources. To generate the farfield spectra, the deconvolved CLEAN maps were integrated with a cutoff of 10 dB from the peak level in the map for each frequency. For illustrative purposes, a sample conventional beamform map at a frequency of 2,250 Hz is displayed in Fig. 4 for the 808 aircraft with the Fowler flaps deflected at 39° and the MLG deployed. To isolate relative source strengths, the maximum SPL has been subtracted from all levels in the map, and a range of 10 dB below the maximum has been used. This convention is also followed throughout the paper, including instances when beamform maps from different datasets are compared. The maximum SPL within a set of maps for a given frequency was subtracted from all levels in the set, and only sources within 10 dB of the maximum are displayed.

As outlined in Ref. [5], two integration regions were used to isolate flap and MLG contributions to the farfield noise and to assess the noise reduction performance of the tested landing gear technologies. These regions are highlighted in Fig. 4: (1) a delta-shaped region named "WingsNg" that excludes the contributions from the nose gear, wing tips and leading edges, and engines; and (2) a small, rectangular region called "MLG" that contains the main landing gears. The "WingsNg" region allowed us to determine the acoustic benefits of the landing gear technologies when the noise produced by the aircraft Fowler flap system was also included in the farfield spectrum. The initial "MLG" region (the smaller rectangular area enclosed by the dash-dot black line) was used to assess the isolated effectiveness of the main gear fairings and cavity treatments by excluding a significant portion of the flap noise. These integration regions were devised to either remove or substantially diminish secondary source contributions to the farfield signature. Nevertheless, as can be seen in Fig. 4, the "MLG" region contains the inboard flap tips, which are known to be prominent noise sources at low- to mid-frequencies, especially when the flaps are highly deflected. Use of the small "MLG" region to partially isolate the main gear noise sources produced inconsistent results: changes in the size and location of the inboard tip noise sources within the beamform maps yielded significantly different integrated spectral levels for repeated flyover passes of the same aircraft configuration. Thus, proper interpretation of the acoustic performance of the tested landing gear technologies became elusive. To circumvent the problem, the initial "MLG" integration region was expanded in the downstream direction (highlighted by the dash-dot red line) to fully enclose the inboard flap tip sources. The integrated levels obtained from the enlarged "MLG" region produced very consistent trends with good data repeatability, as will be shown in the following section. However, this consistency precluded the ability to ascertain the full performance of the tested technologies due to noise contribution from the inboard tip sources. The reasons for choosing the shape and extent of these two integration regions are discussed in Ref. [5]. Unless specified otherwise, the "MLG"-based integrated spectra shown in this paper were obtained from this enlarged integration zone.
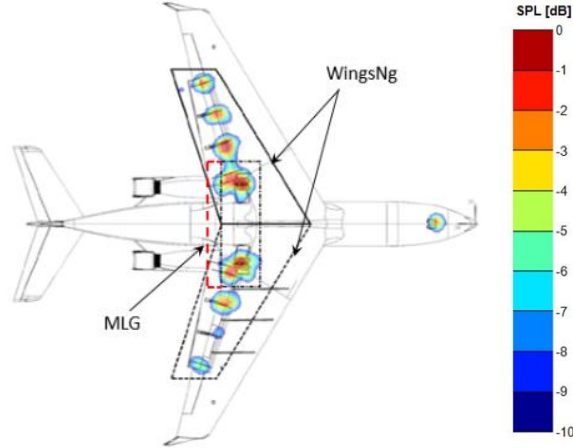
4

Fig. 4 Primary integration regions used to include or exclude contributions of measured sources to the far-field noise spectrum. A sample acoustic map using conventional beamforming is shown (from Ref. [5]).

IV. Results and Discussion

The highest-quality acoustic results were obtained during the time period that corresponded to the aircraft being located along a streamwise segment ± 50 ft from the array center (overhead position). Since the aircraft was closest to the array microphones at this time, atmospheric attenuation and wind-induced decorrelation of high-frequency sound were minimal. Therefore, results corresponding to the overhead position are prominent in the data and analyses presented here. In those instances when the performance of various NR technologies is being examined, data at other angles are also presented to illustrate that the acoustic benefits are maintained over a wide range of forward directivity angles.

A. Data Quality and Repeatability

The extensive acoustic measurements obtained during approximately 1100 flyover passes performed during the 2016 (ARM-I), 2017 (ARM-II), and 2018 (ARM-III) tests permit a careful evaluation of data quality and repeatability in a manner similar to that used during model-scale wind tunnel tests. Although the number of aircraft passes for most configurations was less than that needed for a typical statistical analysis, it was sufficient to ascertain pass-to-pass, day-to-day, and even year-to-year data repeatability. The generation and resultant quality of the beamform maps are discussed in detail in Ref. [5]. Because of the vast amount of data collected during the tests, only a very limited number of beamform maps are presented to demonstrate repeatability of the extracted noise sources or to illustrate the noise reduction capability of the tested technologies. Thus, the analysis is confined to discussing mostly the integrated farfield spectra to highlight the salient trends and features of the collected acoustic data.

1. Velocity Scaling

Velocity scaling is very important during the reduction of data obtained from airframe noise flight tests. Unlike model-scale tests in wind tunnel facilities, exact repetition of target airspeeds is virtually impossible to obtain during actual aircraft flyby passes. Therefore, the resulting spectral levels must be scaled properly for comparison purposes. As in Ref. [5], throughout this paper we have used V^6 velocity scaling to adjust the measured levels. To illustrate the suitability of this scaling, integrated power spectral density (PSD) values at three vastly different speeds for the baseline 804 aircraft with flaps deflected at 20° and landing gear retracted are shown in Fig. 5a. The data were taken during the ARM-III test and the WingsNg region was used to integrate the beamform maps. The corresponding V^6-scaled levels are displayed in Fig. 5b. Good data collapse is observed for frequencies up to 5 kHz, confirming the dependency of flap noise on the assumed velocity scaling. As explained in Ref. [5], the larger variation at frequencies above 5 kHz is caused mainly by residual engine noise, significant atmospheric attenuation of higher-frequency sound waves, and a lower signal-to-noise ratio (SNR) resulting from background/electronic noise. The tight data collapse demonstrated in Fig. 5b unequivocally indicates that V^6 scaling applies uniformly across the entire frequency range of interest. This observation differs from the assumptions used in the semiempirical model of Guo for the prediction of aircraft flap side-edge noise [10], which employs a V^5 dependency at low frequencies and V^6 scaling at high frequencies. The strong V^6 dependency observed in the ARM-III data also differs from the findings of Rossignol [11, 12], who applied Guo's velocity scaling to his model-scale experimental data but obtained a better collapse using $V^{5.5}$ and $V^{6.5}$ scaling at low and high frequencies, respectively.

An even better data collapse was observed for the landing configuration with flaps deflected 39° and landing gear deployed (Figs. 6a and 6b), corroborating similar results presented in Ref. [5] for the 808 aircraft. As has been pointed out in Ref. [5], the 950 Hz tone present at 150 kts was caused by the main gear hollow front post. The intermittency of this tone depends strongly on the aircraft speed and wind direction encountered during a pass.

The main reason for attaining such remarkable data collapse for the landing configuration is the dominance of flap and MLG noise over secondary contributions to the farfield spectrum that may not scale with V^6 (e.g., residual engine noise).

| a) unscaled | b) V^6 scaling applied |
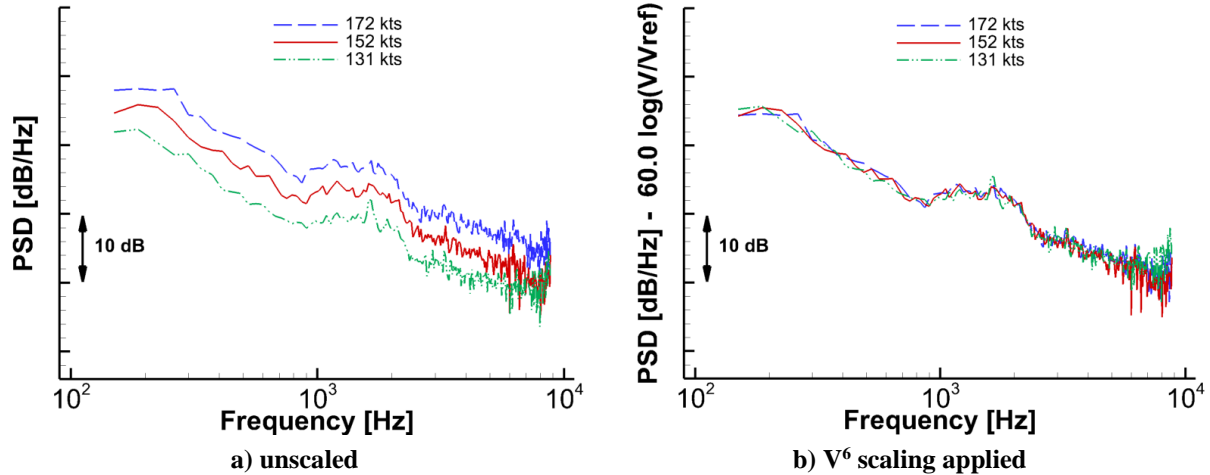
Fig. 5. Noise produced by the 804 aircraft in approach configuration with flaps deflected at 20° and landing gear retracted. Spectra obtained from WingsNg integration of ARM-III test data for overhead position.

| a) unscaled | b) V^6 scaling applied |
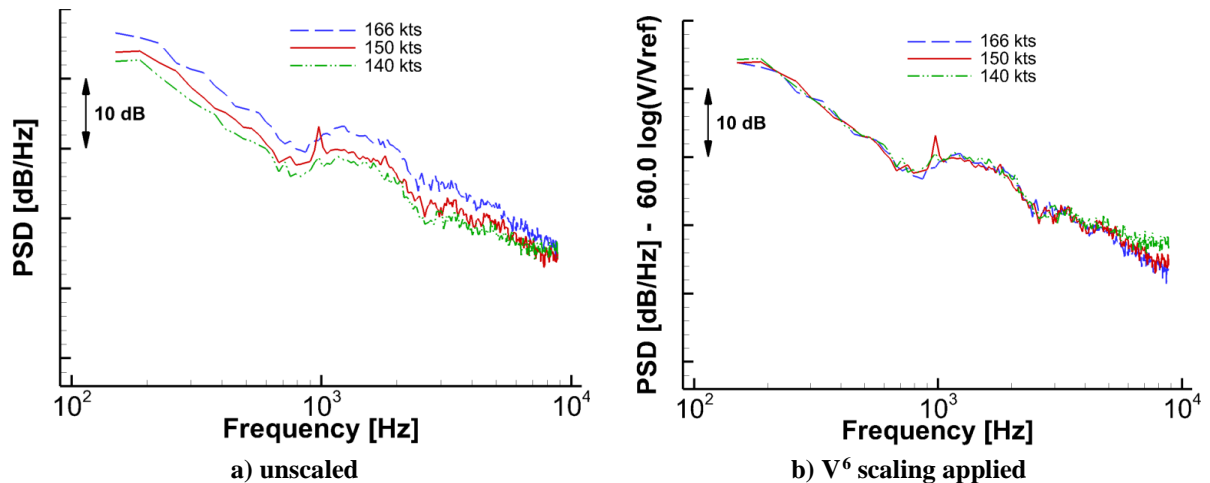
Fig. 6. Noise produced by the 804 aircraft in landing configuration with flaps deflected at 39° and landing gear deployed. Spectra obtained from WingsNg integration of ARM-III test data for overhead position.

2. Data Consistency

Consistency of the acoustic measurements from repeat aircraft passes is discussed in this section. Sample 1/12th-octave beamform maps from passes of the 804 aircraft with flaps deflected 39° and landing gear deployed are shown in Fig. 7 at three select frequencies representative of low-, medium-, and high-frequency noise content. This configuration was used as a baseline for determining the performance of the main gear NR technologies. The sound levels have been scaled to 150 kts based on V^6. The noise maps have also been normalized for each figure by subtracting the maximum SPL at each frequency from the corresponding contours, thus allowing a direct comparison for the location, strength, and shape of the noise sources. The maps in the left and middle columns correspond to two consecutive aircraft passes (no. 4 and 5) executed during March 20, 2018 and those on the right column belong to pass no. 9 executed on March 30, 2018. At the frequency of 375 Hz, all three maps indicate that the main gear cavity and flap inboard tips are the prominent sources. At 2,000 Hz, the major sources are the main and nose gears as well as the

inboard and outboard flap tips. Notice that, at medium frequencies, the flap brackets are also important secondary sources. At the high frequency of 4,500 Hz, the flap inboard tips appear as the dominant sources, followed by the main and nose landing gears as much weaker sources. Overall, the maps show that all three passes produce a consistent identification of the airframe noise sources with peak sound levels in the maps that fall within 1-2 dB of each other. Although not shown here, careful inspection of the maps at most other frequencies indicates a similarly close agreement. Inspection of the maps reveals minor differences in the shape and peak level of the noise sources on either side of the aircraft. Such subtle discrepancies are to be expected and are mostly attributed to the uncontrolled nature of the test environment during the aircraft flyovers.

a) f = 375 Hz　　　　　　b) f = 375 Hz　　　　　　c) f = 375 Hz

d) f = 2,000 Hz　　　　　　e) f = 2,000 Hz　　　　　　f) f = 2,000 Hz

g) f = 4,500 Hz　　　　　　h) f = 4,500 Hz　　　　　　i) f = 4,500 Hz

I) Pass no. 4, March 20, 2018　　**II) Pass no. 5, March 20, 2018**　　**III) Pass no. 9, March 30, 2018**

SPL [dB]

-10　-9　-8　-7　-6　-5　-4　-3　-2　-1　0
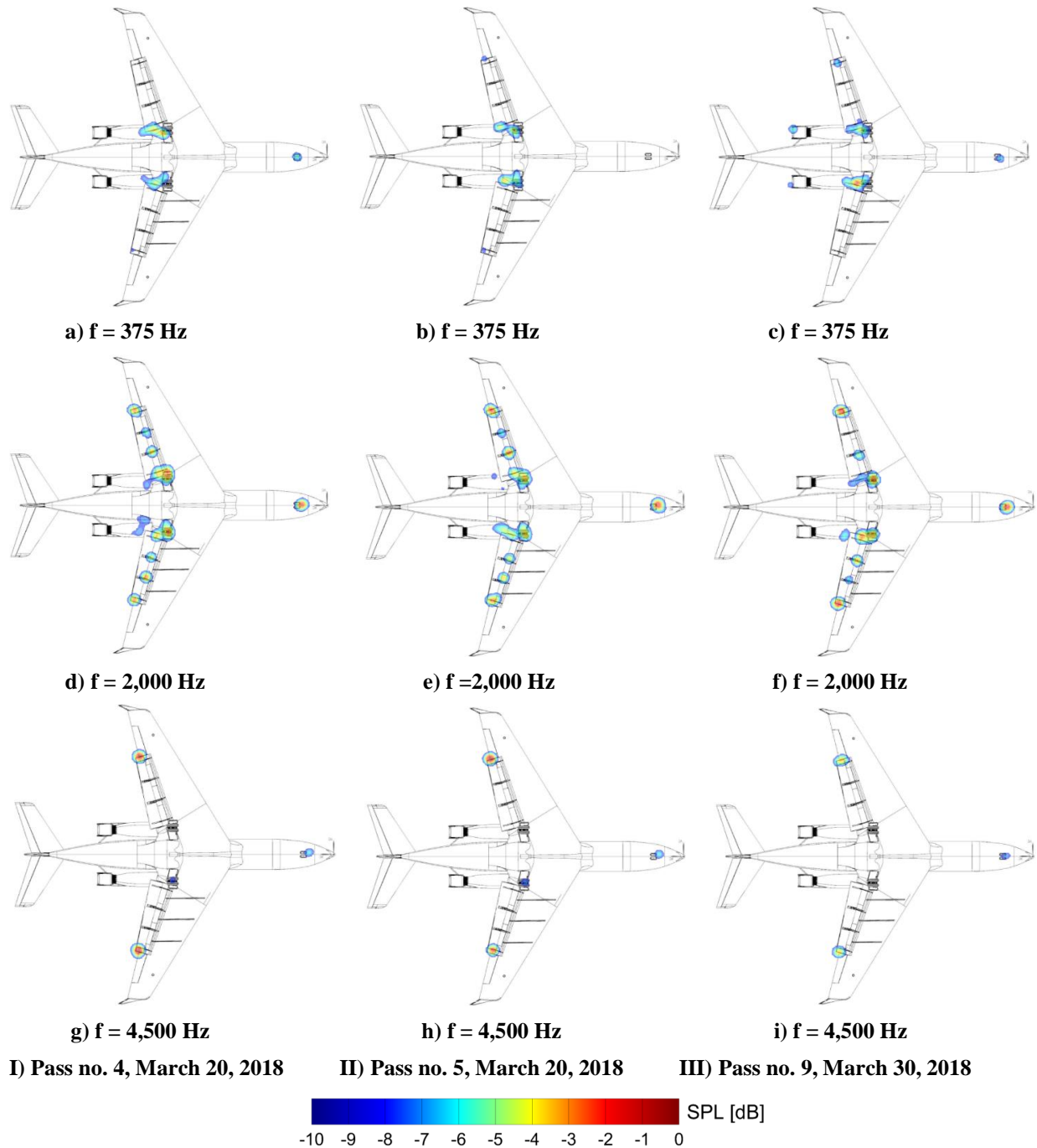
Fig. 7. Beamform maps for the 804 aircraft in landing configuration with flaps deflected at 39° and landing gear deployed at overhead position.

3. Data Repeatability

To assess the repeatability of the acquired acoustic data, we utilize the integrated PSD plots associated with the 808 aircraft. Despite the lack of measured true air speed (TSA) and reliance on IAS (as called out by the pilots) for scaling purposes, this aircraft was extensively tested during all three ARM deployments. As such, the gathered measurements provide a wealth of data for examining pass-to-pass repeatability, consistency of the observed trends, and data quality that spans multiple years and test sites. In Fig. 8, we present the integrated spectra based on the "WingsNg" region for the 808 configuration with flaps deflected 20° and landing gear retracted. The plotted dataset contains 3 passes from ARM-I (2016), 9 passes from ARM-II (2017), and 5 passes from ARM-III (2018). The figure illustrates that all the passes produced consistent spectral levels that approximately fall within a 3 dB band. To isolate the trends, averaged spectra based on p^2 averaging of all the passes from each year were generated and the results are plotted in Fig. 9. Also included in Fig. 9 is the averaged spectrum for all shown multiyear passes. Except for a narrow frequency band between 700 Hz $<$f $<$ 1,000 Hz, there is very good agreement among all averaged spectra up to 5–6 kHz, indicating that the measurements are highly consistent and repeatable. The underlying factors causing the discrepancies at higher frequencies are the same as those mentioned previously. The differences occurring in the frequency band 700 Hz $<$ f $<$ 1,000 Hz are puzzling, as no changes were made to the aircraft nor the test procedure. Moreover, the averaged spectra from the 2016 and 2018 passes are almost coincident, with the 2017 averaged spectrum being noticeably higher. Therefore, differences in the spectral levels cannot be attributed to the change in test site nor to the microphone array being deployed on a concrete-paved surface. We will examine this issue further when results from the 39° flap deflection are presented. For ease in visualization of the results, only the averaged spectra are presented for the other 808 aircraft configurations.
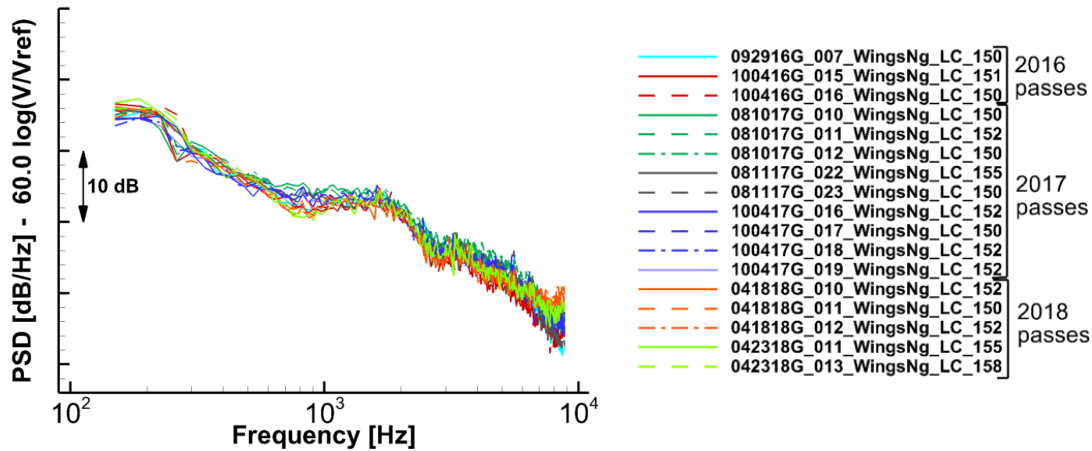

Fig. 8. Passes spanning multiple years for the 808 aircraft in approach configuration with flaps deflected 20° and landing gear retracted. Spectra from WingsNg integration for overhead position.
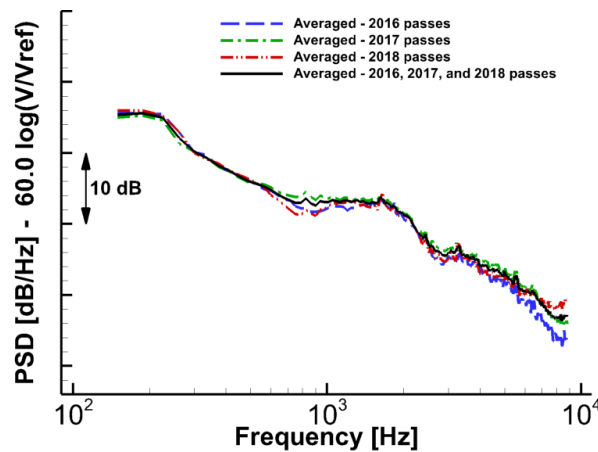

Fig. 9. Averaged spectra for the 808 aircraft in approach configuration with flaps deflected 20° and landing gear retracted. Spectra from WingsNg integration for overhead position.

Multiyear averaged spectra for the 808 aircraft with flaps deflected 20° and landing gear deployed are shown in Fig. 10. The spectra display very good agreement with each other and with the averaged levels obtained from all the aircraft passes. Apart from the expected differences at high frequencies, the most noticeable discrepancy occurs in the 600 Hz < f < 1,000 Hz range, where the averaged spectrum from 2017 possesses higher levels. The averaged spectra for the 808 aircraft in the landing configuration of 39° flap deflection with landing gear retracted and deployed are presented in Figs. 11a and 11b, respectively. Remarkable agreement between the 2016, 2017, and 2018 results is observed. Again, the most notable discrepancy occurs in the 600 Hz < f < 1,000 Hz range. Compared to the 20° flap deflection, the differences in spectral levels at this higher flap deflection coincide with the appearance of a moderate tonal hump centered around 785 Hz. Examination of sample 1/12th-octave beamform maps from 2017 and 2018 passes in the 750 Hz < f < 900 Hz frequency band indicates that the tonal noise is generated at the flap inboard edges. The only geometric feature capable of producing such a noise source is the 0.5" (1.25 cm) deep cavity at both inboard and outboard tips. The shallow cavity begins at the flap leading edge and extends over most of the flap chord. With increasing flap deflection, flow angularity at the flap side-edge causes a more normal, rather than parallel, impingement of incoming flow on the cavity. As a result, the separated flow at the bottom edge of the cavity interacts with the top edge and generates the tone. Although the presence of the cavity explains the appearance of the tone, it does not answer why it would consistently produce higher-amplitude noise during the 2017 passes than similar passes in 2018 or 2016.
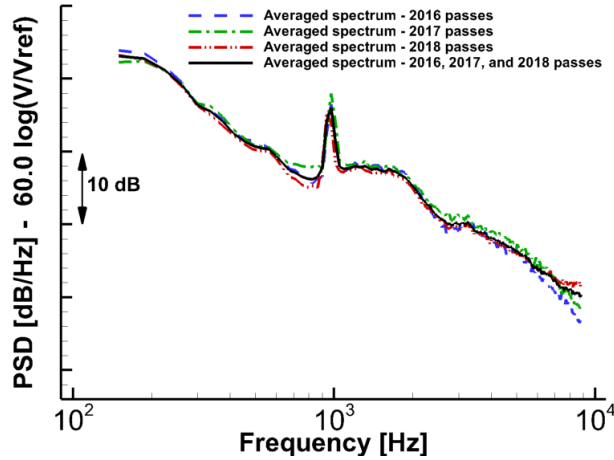

Fig. 10. Averaged spectra for the 808 aircraft in approach configuration with flaps deflected 20° and landing gear deployed. Spectra from WingsNg integration for overhead position.

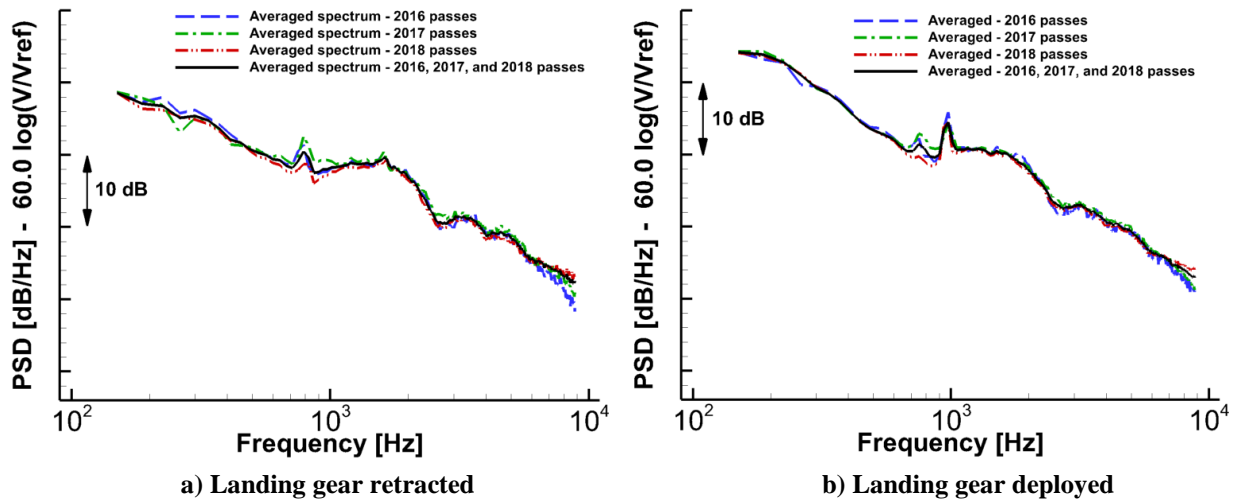a) Landing gear retracted

b) Landing gear deployed

Fig. 11. Averaged spectra for the 808 aircraft for flaps deflected 39° with landing gear retracted and deployed. Spectra from WingsNg integration for overhead position.

The 804 aircraft in its conventional Fowler flap configuration without treatments on the gear or wheel cavity (baseline configuration) was only tested during the ARM-III test (2018). Therefore, a similar year-to-year data repeatability analysis cannot be conducted for this testbed. However, there are two 804 configurations that can be used to assess yearly data consistency. In Fig. 12a, integrated spectra based on the WingsNg region for passes of the 804 aircraft conducted in 2016 and 2018 are compared. The 2016 passes (dash-dot blue lines) used ACTE flaps set at 0° (cruise configuration) and landing gear deployed. The 2018 passes (solid red lines) were conducted with 804 Fowler flaps set at 0° deflection (cruise wing) and landing gear deployed. Notice that the two sets of data collapse nicely within a narrow amplitude band, indicating that the measurements were consistent and repeatable. The spectra obtained from averaging the passes for each year and the passes for the two years are presented in Fig. 12b. Good correspondence among the spectra is observed. The slightly higher jitter in the averaged levels for the 2018 data is attributed to the low number of passes available for averaging.

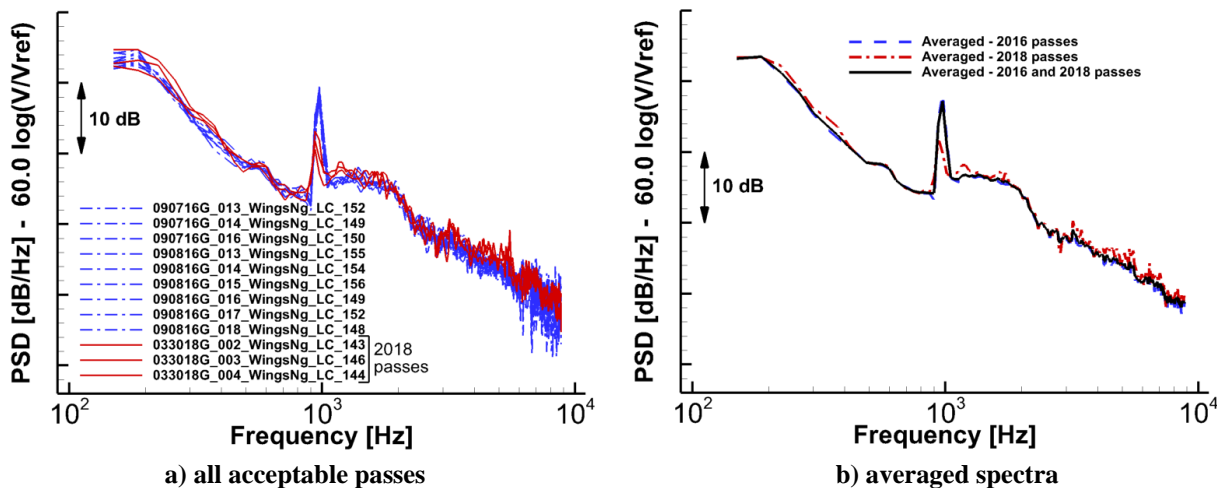a) all acceptable passes

b) averaged spectra

Fig. 12. Passes spanning multiple years for the 804 aircraft for flaps deflected 0° and landing gear deployed. Spectra from WingsNg integration region for overhead position.

We now demonstrate that good consistency in the gathered data should be expected when NR technologies for the main gear are applied. Spectra from integration of data within the MLG region obtained during flyovers of the 804 aircraft with ACTE (2017) and Fowler (2018) flaps set at 0°, with fairings and cavity mesh installed on the main landing gear during both flights, are plotted in Fig. 13. Data from 2017 (804 with ACTE) passes are represented by dash-dot blue lines; data from 2018 (804 with Fowler) passes are identified by solid red lines. Highly consistent and repeatable trends for the two sets of passes are observed, producing averaged spectra that are very similar in shape and levels.

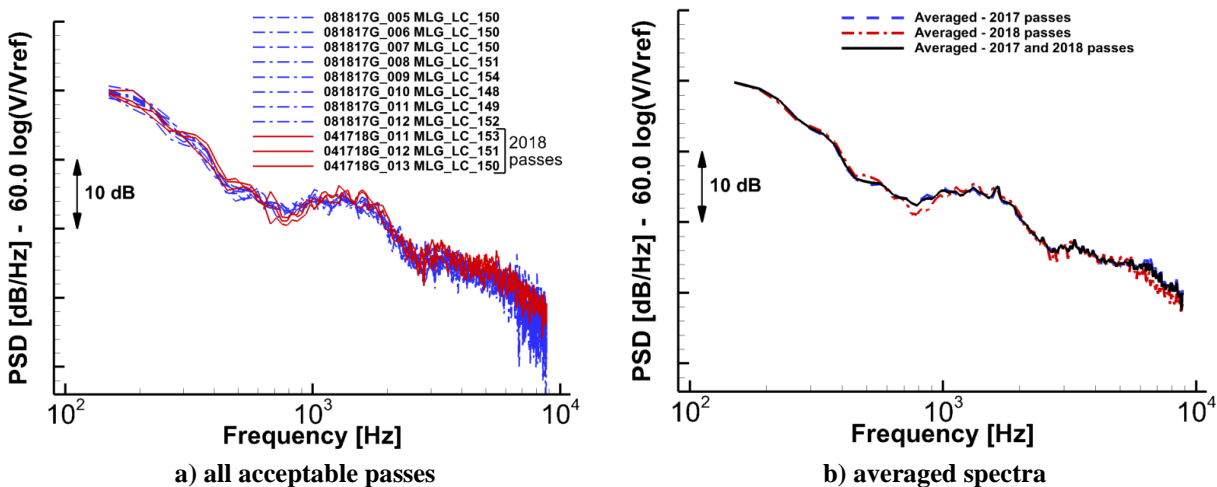a) all acceptable passes

b) averaged spectra

Fig. 13. Passes spanning multiple years for the 804 aircraft with 0° deflected flaps and fairings and cavity mesh applied to main landing gear. Spectra from MLG integration region for overhead position.

10

4. Impact of Local Meteorological Conditions

The impact of local meteorological conditions on the quality and repeatability of the measurements is assessed in this section. The results presented here complement earlier analyses of ARM-I and ARM-II data regarding this important issue [8]. For this discussion, we relied exclusively on ARM-III (2018) data for two critical configurations with the most repeat flights. MLG region integrated spectra for all acceptable passes[5] of the 804 aircraft with flaps deflected 39° and fairings plus cavity chevrons and foam applied to the main landing gear are shown in Fig. 14. The aircraft passes were performed on different days with good combinations of temperature and relative humidity. Low winds (1.9 m/s) were encountered on April 3, relatively high winds (4.5 m/s) on April 5, and moderate winds on April 30 (2 to 3.5 m/s). Figure 14 shows a tight collapse of the spectra that fall within 2 dB of each other. Excellent day-to-day repeatability of the acquired acoustic measurements is demonstrated by the averaged spectra for each day, plotted in Fig. 15. Also included in this figure are the average of all acceptable passes collected during the three days and the average of five select passes from the same days. These five spectra were chosen because aircraft AOA, glide slope, fuel weight, and position above microphone array closely matched. For frequencies below 5 kHz, there are hardly any differences among the averaged spectra, indicating that good local meteorological conditions alone could be essential to obtaining good quality measurements. The fact that the averaged spectrum from the five select passes coincides with the other averages provides insight on the dependencies of airframe noise on aircraft parameters – during approach or landing, the farfield noise footprint is very weakly dependent on aircraft AOA, glide slope, and weight. The extremely weak dependency on AOA observed here corroborates the model-scale test results of Ref. [13].
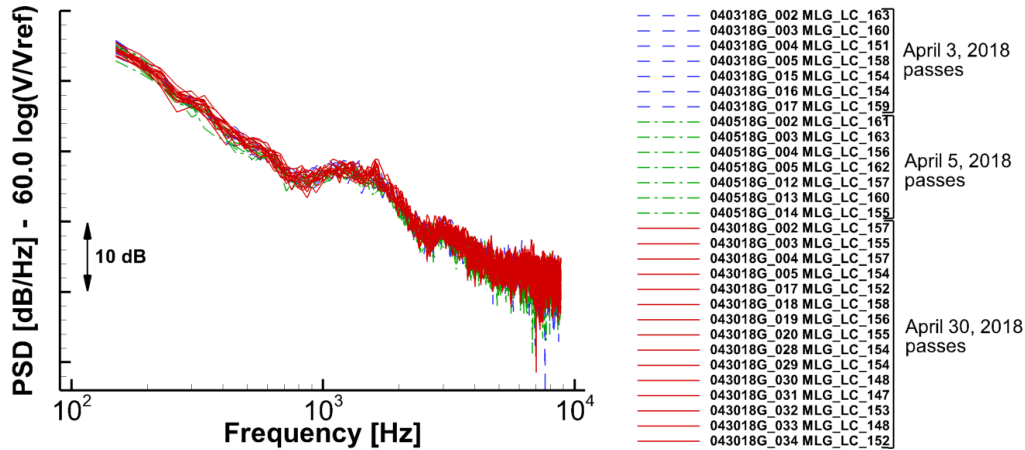

Fig. 14. Integrated spectra for 804 aircraft with flaps deflected at 39° and fairings plus cavity chevrons and foam applied to main landing gear. Spectra from MLG integration region for overhead position.
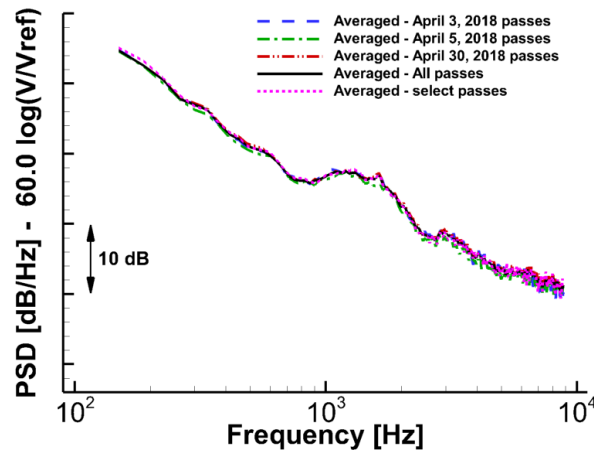

Fig. 15. Averaged spectra for the 804 aircraft with flaps deflected at 39° and fairings plus cavity chevrons and foam applied to main landing gear. Spectra from MLG integration region for overhead position.

---

[5] See Ref. [5] for definition of pass acceptance.

The quality of acoustic data obtained on days with good local meteorological conditions was demonstrated in Figs. 14 and 15. We will now explore the behavior of farfield noise when acoustic data were acquired under less than optimal meteorological conditions. Integrated spectra based on the WingsNg region are presented for the 804 aircraft in the landing configuration (flaps deflected 39° and landing gear deployed) in Fig. 16. Measurements for this configuration were obtained during five days. The temperature-relative humidity conditions were excellent for the three days in March. The winds were low to moderate, and more importantly, steady during these three days with March 30 being one of the best test days of the ARM-III deployment. The temperature-relative humidity combinations for the two test days in April were marginal, combined with fluctuating winds (relatively high atmospheric turbulence) even though overall wind magnitude remained moderate (1 minute averages less than 2.5 m/s) and within the acceptable range. The passes conducted on March 20, 29, and 30 produced very similar spectral content, as seen in Fig. 16. Spectra from the April 21 passes (dark blue dash-dot lines) are consistent but show noticeably lower amplitudes than the spectra collected during the three days in March. The differences in amplitude increase with frequency because of higher atmospheric attenuation and decorrelation of the sound waves caused by wind gusts. As clearly shown in Fig. 16, the worst results were obtained during April 24 and show even larger differences with the spectra from data acquired during March. The corresponding daily averages are presented in Fig. 17. The low number of passes available for March 20 and 29 prompted consideration of the March data under a single grouping. There are significant differences in the daily averaged spectral levels, with the April 24 averaged spectrum showing 2–4 dB lower levels at medium and high frequencies. Also included in Fig. 17 is the averaged spectrum composed of passes from all days. Although this spectrum lies closer to the averaged spectrum for the March passes, differences on the order of 1 to 1.5 dB are still present. Although these differences may seem reasonable, they have a devastating effect when trying to assess the performance of landing gear noise abatement technologies, where the maximum reductions that can be obtained are on the order of 3–4 dB at most frequencies. As the results in Fig. 17 clearly demonstrate, the availability of data from multiple flight days is essential for critical aircraft configurations of interest, in particular for those configurations that will serve as baselines. Since there is no viable correction for the severely adverse effects that gusty winds have on medium and high frequency noise, testing should be performed during days when both steady and fluctuating winds are low even if the temperature-relative humidity combinations are marginal. Based on the results shown in Fig. 17, only the averaged spectrum obtained from the March passes was used as the baseline to determine the noise reduction performance of various gear technologies discussed in section IV-B.
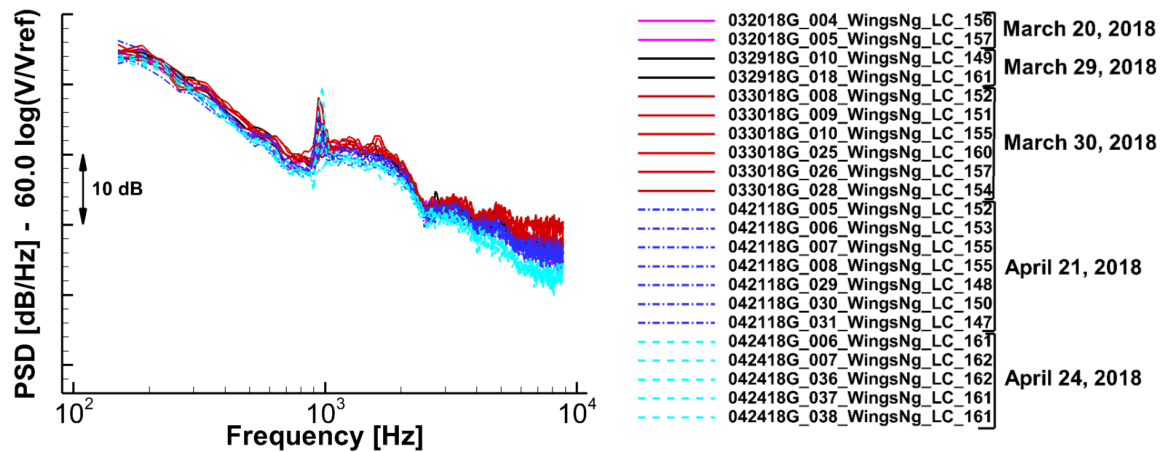

Fig. 16. Integrated noise spectra for 804 aircraft with flaps deflected 39° and landing gear deployed. Spectra from WingsNg integration region for overhead position.
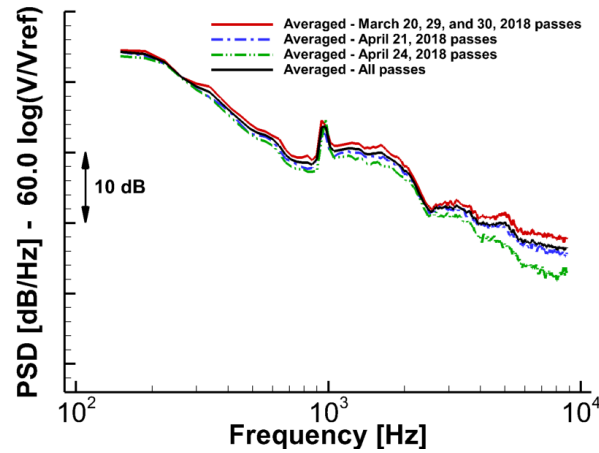
Fig. 17. Averaged spectra for the 804 aircraft with flaps deflected 39° and landing gear deployed. Spectra from WingsNg integration region for overhead position.

5. Effect of Baseline Aircraft on Farfield Noise

This section addresses whether the 804 and 808 aircraft in their conventional Fowler flap (baseline) configuration produce similar farfield noise signatures. Due to the unavailability of baseline 804 data at the time, the noise reduction performance of the ACTE flap with and without MLG noise abatement technologies was evaluated in Ref. [5] using data acquired during the ARM-I and ARM-II flights with the 808 aircraft as the baseline. Integrated spectra from the WingsNg region for three select passes for each aircraft from the ARM-III (2018) campaign are plotted in Fig. 18a. Since the 808 aircraft is not instrumented, fuel weight was used to match 804 and 808 passes. As seen clearly in Fig. 18, correspondence between the farfield noise signatures of the two aircraft is very good for frequencies up to 5 kHz. Beyond 5 kHz, the 804 aircraft is noisier. As demonstrated in Ref. [5], the extra noise is produced by the 804 engines, which are older and use a different generator cooling system than the 808 engines. The observed agreement becomes more remarkable when considering that only IAS values (as called out by the pilots) were used to scale the 808 spectral levels. Averaged spectra for the two aircraft, obtained from all acceptable passes executed during ARM-III, are shown in Fig. 18b. Also plotted in this figure are the averaged spectra for the select passes of Fig. 18a. For frequencies up to 5 kHz, the averaged spectra fall within a very tight band. Beyond 5 kHz, 804 engine noise causes higher spectral levels. However, as described in Refs. [5, 8], the quality of the measured signal deteriorates very rapidly for frequencies above 5 kHz. The causes are atmospheric attenuation, poorer SNR due to background and electronic noise, and residual engine noise. Thus, for the purposes of evaluating the performance of the airframe technologies tested, one can assume that the noise signatures of both aircraft in their baseline configuration are equivalent. As a result, there is no need to reevaluate the airframe technologies presented in Ref. [5] using baseline 804 data collected in 2018.
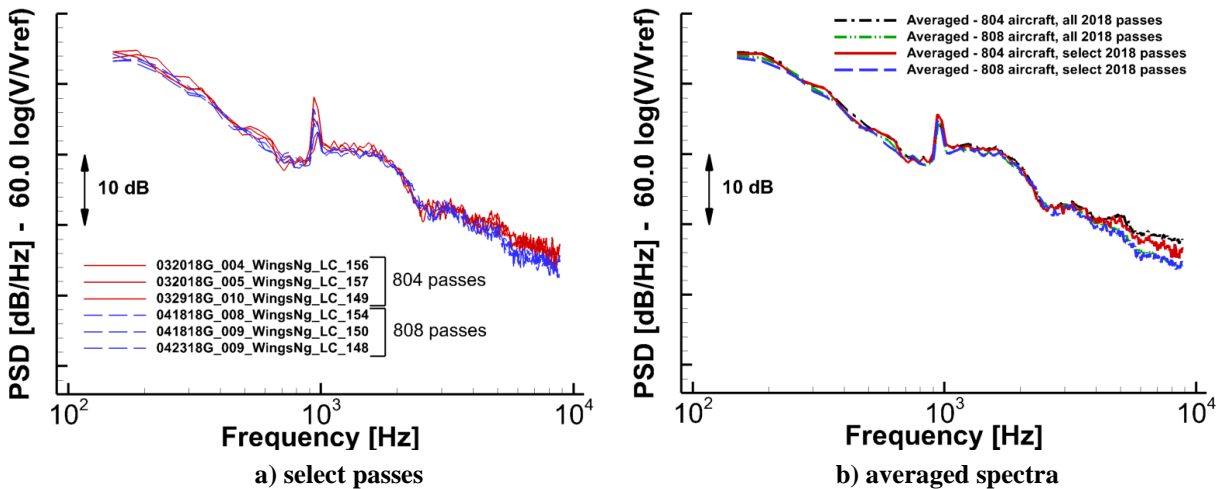

a) select passes

b) averaged spectra

Fig. 18. Individual and averaged spectra for 804 and 808 aircraft with 39° deflected flaps, landing gear deployed. Spectra from WingsNg integration region for overhead position.

13

B. Performance of Landing Gear Noise Reduction Technologies

Since a vast amount of data was gathered during the ARM-III test, we include here only a few representative beamform maps that demonstrate how the applied technologies affected the intended noise sources. Because of the prominence of the inboard tip source at high flap deflection angles, the 20° deflection was used to highlight the true noise reduction potential of the gear treatments. Sample CLEAN beamform maps for the 804 aircraft with its Fowler flaps deflected 20° without (baseline) and with MLG NR technologies are displayed in Fig. 19 at low, medium, and high frequencies for the overhead position. For the treated gear configuration, the installed NR technologies comprised the MLG fairings plus cavity chevrons and sound absorbing foam. This combination represents the quietest configuration tested. For frequencies below 600 Hz, the MLG cavity is the dominant source with the main gear acting as a secondary source [5]. Comparison of the maps at 450 Hz (shown in Figs. 19a and 19b) clearly demonstrates that the gear fairings and cavity treatment significantly reduce the noise generated by the MLG, lowering peak sound levels by approximately 6 to 7 dB. At mid-frequencies (Figs. 19c and 19d), the noise benefit is slightly less, approaching 4 to 5 dB, since cavity noise is no longer a major contributor and reductions are produced mostly by the gear fairings. As shown in Figs. 19e and 19f, the fairings also perform exceptionally well at higher frequencies. The corresponding impact on integrated noise levels is presented later in this section.

Similar maps for the same two aircraft configurations at a 39° flap deflection are presented in Fig. 20. For this higher deflection angle, at low and medium frequencies, the inboard flap tips are prominent sources comparable in strength to the cavity and MLG sources (Figs. 20a, 20c, and 20e). As was the case for the lower flap deflection, the maps vividly illustrate that at 39° the cavity treatments and gear fairings successfully either eliminate or greatly diminish the strength of the MLG noise sources (Figs. 20b, 20d, and 20f) without affecting the inboard tip sources. For frequencies greater than about 3 kHz, the flap outboard tips become the dominant airframe sources and mask the noise reduction potential of the gear technologies.
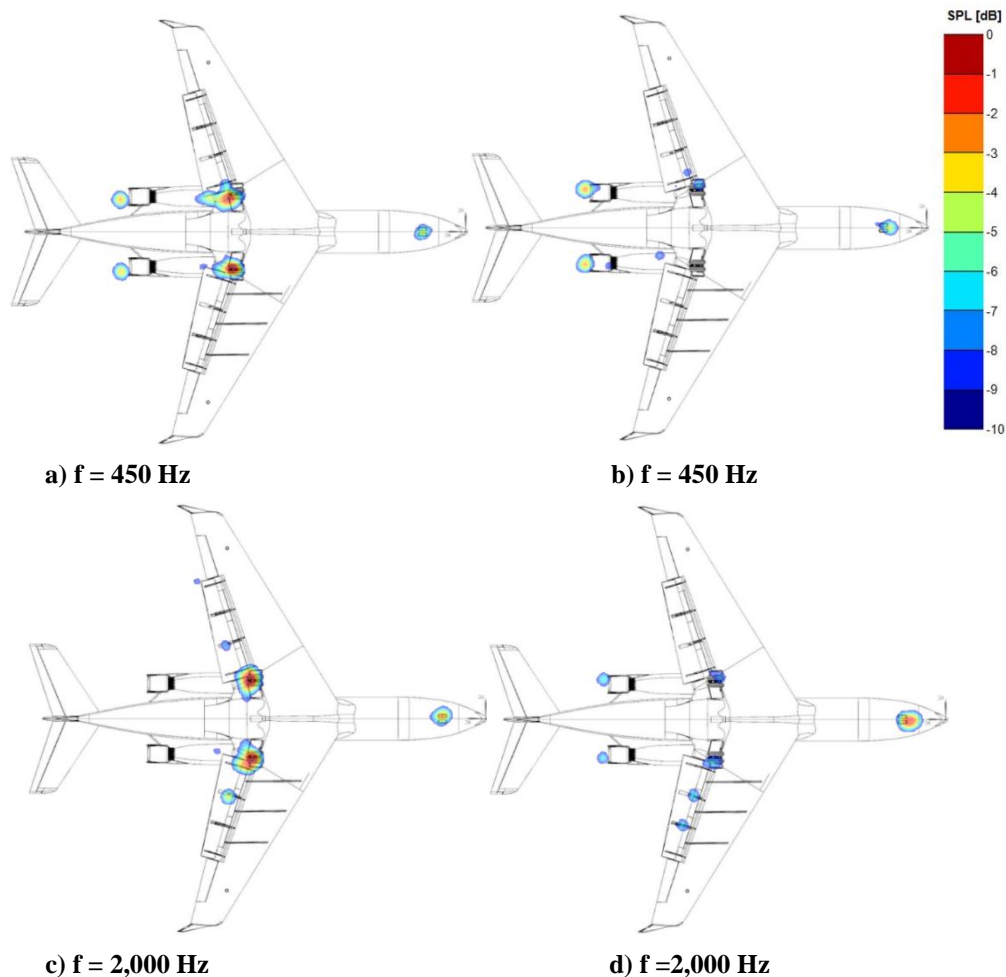

a) f = 450 Hz   b) f = 450 Hz

c) f = 2,000 Hz   d) f = 2,000 Hz

Fig. 19. Noise produced by 804 with Fowler flaps deflected 20°, without (left column) and with (right column) NR technologies installed – MLG fairings plus cavity chevrons and foam. Overhead position.
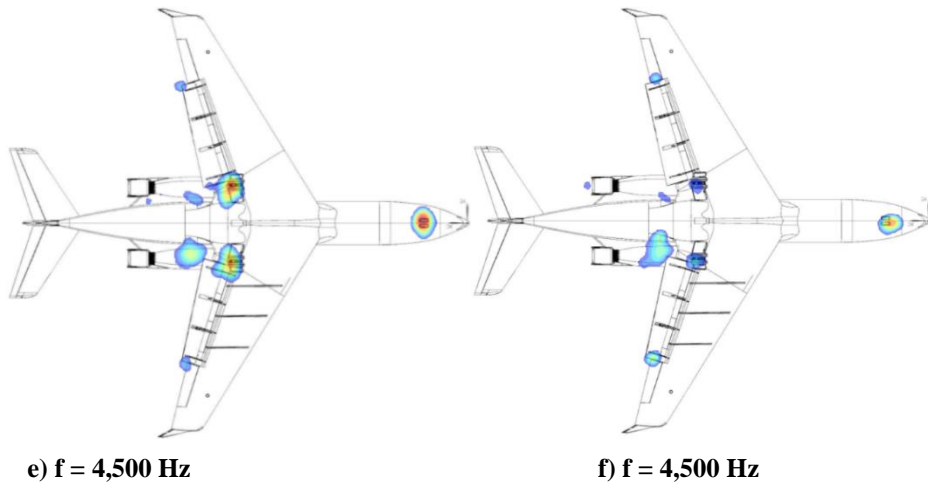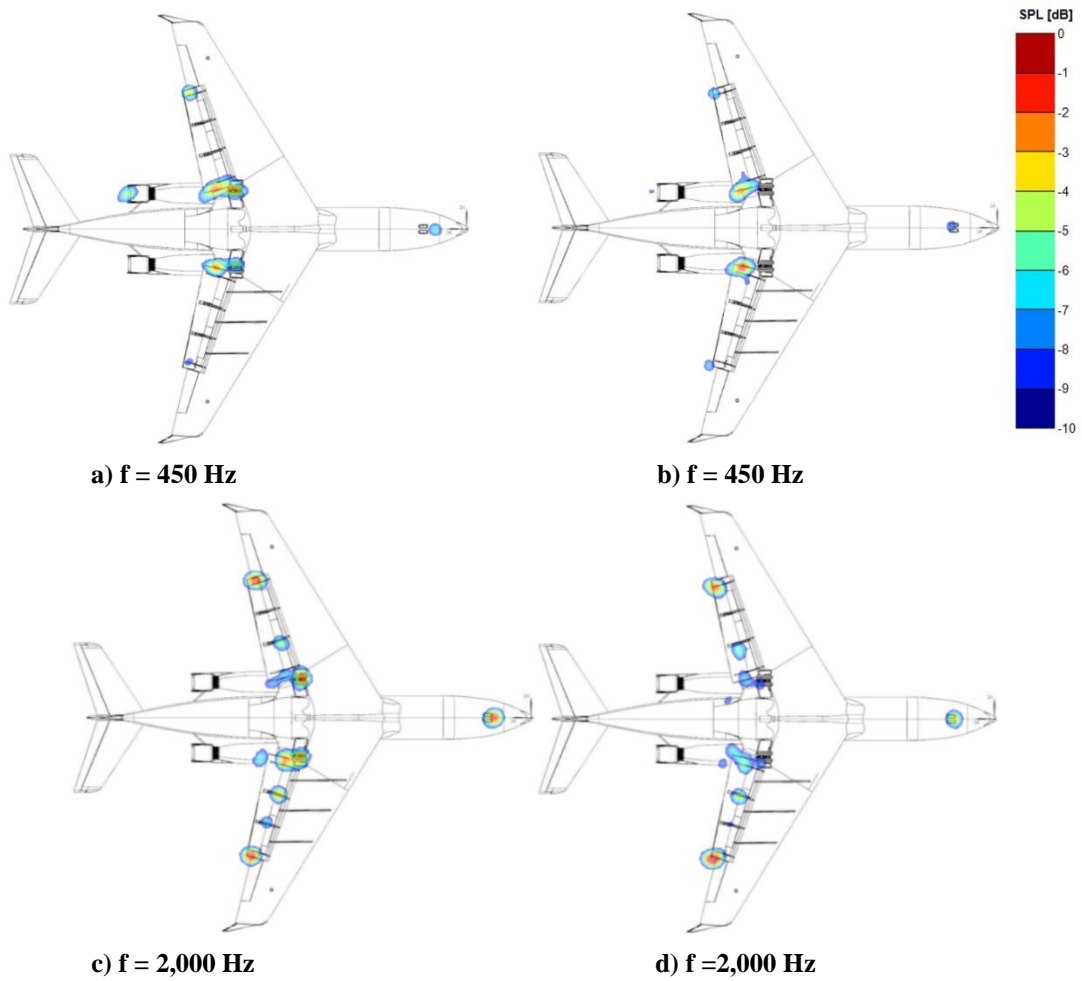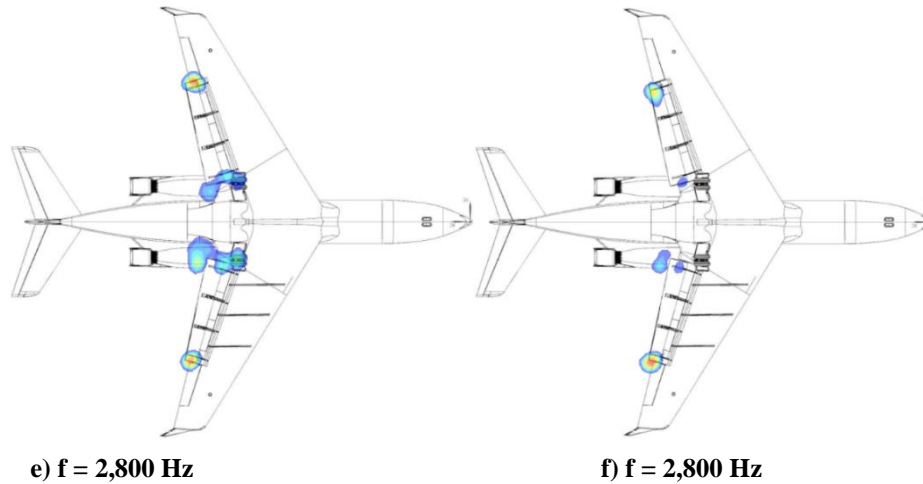
14

e) f = 4,500 Hz   f) f = 4,500 Hz

Fig. 19. Concluded.

a) f = 450 Hz   b) f = 450 Hz

c) f = 2,000 Hz   d) f =2,000 Hz

Fig. 20. Noise produced by 804 with Fowler flaps deflected 39°, without (left column) and with (right column) NR technologies installed – MLG fairings plus cavity chevrons and foam. Overhead position.

e) f = 2,800 Hz　　　　　　　　　　　　　**f) f = 2,800 Hz**

Fig. 20. Concluded.

　　To accurately extract the noise reduction attained with the MLG technologies, the "MLG" region was used for integrating the CLEAN beamform maps. The averaged (for multiple passes), integrated, overhead farfield spectra corresponding to the untreated (baseline) and several configurations with treated MLG are presented in Fig. 21 for a flap deflection of 20°. The plotted spectra demonstrate and quantify the acoustic benefits achieved with the installed MLG technologies – significant noise reduction that is maintained over the entire frequency range. Notice that significant jitter is present in the spectra at frequencies above approximately 5 kHz. The highest noise reduction was achieved with the combination of the gear fairings plus cavity chevrons and foam. Due to the much lower magnitude of noise generated at the inboard tips for this flap deflection, the integrated spectra using the MLG region captures a substantial portion of the noise reduction benefits attained with the applied technologies. This combination of the technologies produces close to 5 dB reduction at frequencies below 400 Hz and 3-4 dB for higher frequencies. The reduction levels reported here are slightly less than the values reported in Ref. [5] for an ACTE-equipped 804 aircraft when the flap noise was virtually eliminated. As seen in Fig. 21, the combination of the gear fairings plus cavity mesh provides less noise benefits for frequencies below 2 kHz. The removal of chevrons from the cavity (i.e., fairings plus foam installed) results in less noise reduction only in the 200 Hz < f < 400 Hz range. Otherwise, the integrated spectrum is nearly the same as that produced by the fairings plus chevrons and foam combination. The configuration involving only gear fairings lacks the full reduction benefits at lower frequencies. Nevertheless, the fairings still deliver in excess of 1 dB reduction at frequencies below 300 Hz. At higher frequencies, the fairings produce close to 3 dB reduction that is about 1 dB less than the fairings plus foam combination. As alluded to in Ref. [5], this difference suggests that the beneficial effects of placing sound absorbing foam on the back wall of the gear cavity is not limited to the very low frequency end of the spectrum. Surprisingly, good noise reduction was delivered by the combination of cavity chevrons and foam. Without the gear fairings, we anticipated a rapidly diminishing performance for this combination at frequencies above 900 Hz to 1 kHz. However, as the averaged spectrum in Fig. 21 indicates, substantial reduction was achieved over most of the frequency range of interest. The flyover passes for this configuration were executed during a single test day when local meteorological conditions were marginal with moderate winds. Therefore, one must assume that the integrated levels at medium to high frequencies come with a higher degree of uncertainty in the collected data.

　　Airframe noise is known to be dominant in the forward directivity angles. To demonstrate that the performance of the gear technologies is maintained over a large segment of the forward quadrant, integrated averaged spectra at directivity angles of ~67° and ~45° are presented in Fig. 22a and 22b, respectively. The data show similar, or even larger, reductions at these additional directivity angles. Good performance over a wide range of directivity angles typically translates into a substantial reduction in effective perceived noise levels (as demonstrated in Ref. [14]), a key metric for acceptance of new technologies by the industry. The averaged spectra for the same combinations of the gear NR technologies for the 804 aircraft with Fowler flaps set at 39° are presented in Fig. 23. As expected, noticeably lower reductions are observed for all tested technology combinations due to the fact that integration of the MLG region now contains contributions from inboard flap tip sources that mask the true performance of the gear and cavity technologies. Despite this contamination, a reduction on the order of 2 to 3 dB was indicated by the measured data. As was the case for the flaps deflected 20°, the noise benefits become somewhat larger at forward directivity angles with the combination of gear fairings plus cavity chevrons and foam still providing the best performance.
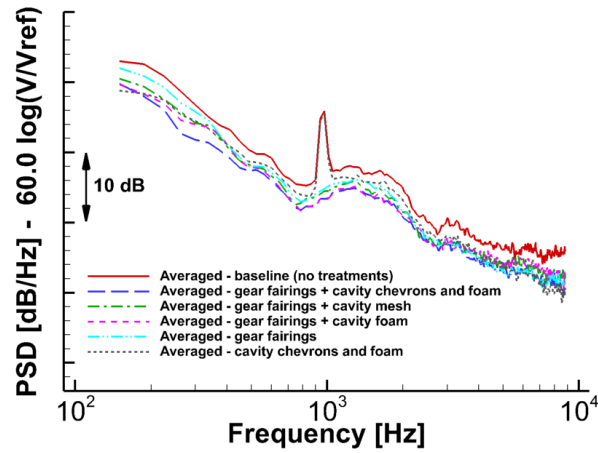
16

Fig. 21. Averaged spectra from 804 passes for Fowler flap 20°, gear deployed without/with various combinations of MLG treatments installed. Spectra from MLG integration region for overhead (90° directivity angle).
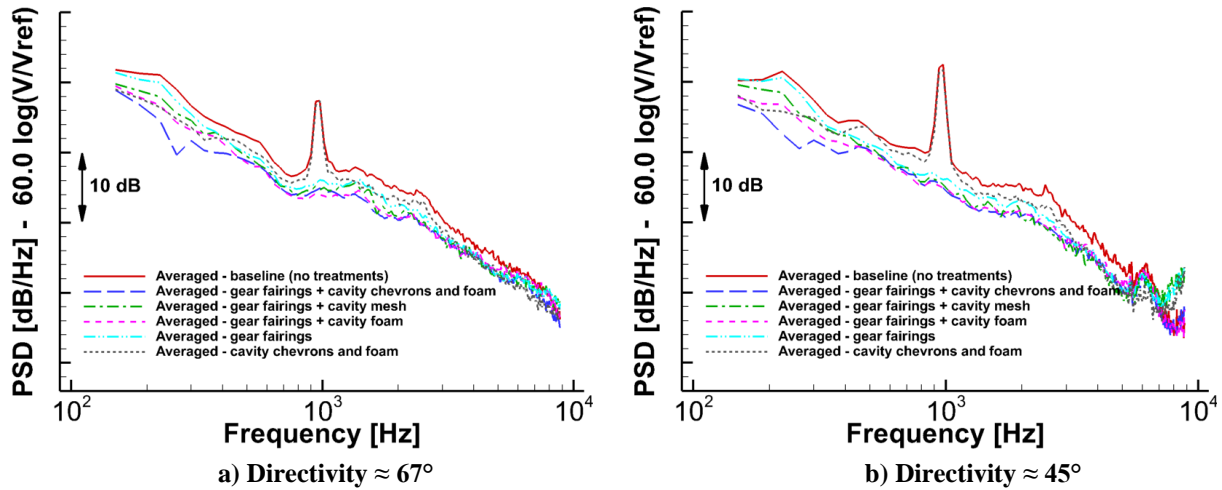

a) Directivity ≈ 67°

b) Directivity ≈ 45°

Fig. 22. Averaged spectra from 804 passes for Fowler flap 20°, gear deployed without/with various combinations of MLG treatments installed. Spectra from MLG integration region at forward directivity angles.
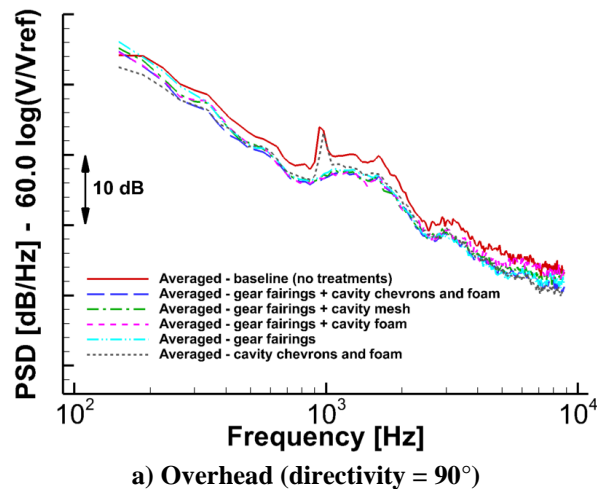

a) Overhead (directivity = 90°)

Fig. 23. Averaged spectra from 804 passes for Fowler flap 39°, gear deployed without/with various combinations of MLG treatments installed. Spectra from MLG integration region at overhead and forward directivity angles.
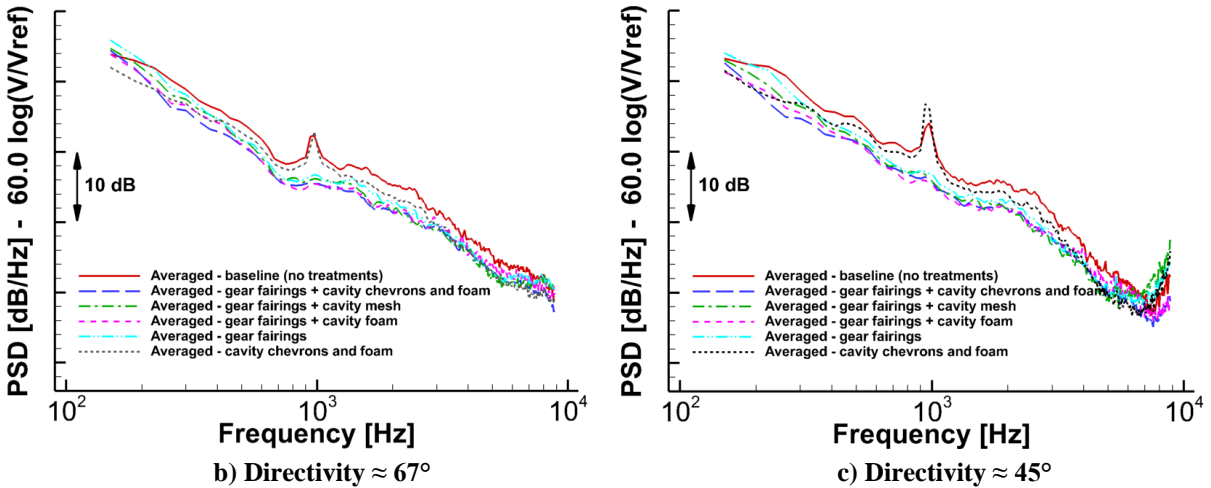
b) Directivity ≈ 67°

c) Directivity ≈ 45°

Fig. 23. Concluded.

V. Concluding Remarks

Detailed aeroacoustic analyses of phased microphone array data obtained during flyover passes conducted for the 2018 ARM-III flight test were presented in this paper. The goal of the test was to evaluate the acoustic performance of main landing gear and cavity noise abatement technologies installed on a Gulfstream G-III aircraft flying in its conventional (Fowler) flap configuration. Microphone array measurements from the 2018 test, combined with acoustic data collected during the 2016 (ARM-I) and 2017 (ARM-II) tests were used to study the quality and consistency of the acquired measurements. Through careful examination of data from numerous aircraft passes obtained on multiple flight days and spanning three years, good collapse of the integrated farfield noise spectra was demonstrated, establishing excellent year-to-year repeatability of the measured trends. The good collapse highlighted the fact that airframe noise is only mildly dependent on the aircraft angle of attack, glide slope and fuel weight, and atmospheric corrections for temperature/humidity are effective even for marginal conditions. However, high winds or elevated wind fluctuations produced uncorrectable and unacceptable data variability. The analyses also indicated that, for any of the tested configurations, the spectrum obtained from p^2 averaging all the acceptable repeat passes is representative of the overall spectral content levels, but this requires sufficient passes to identify and exclude outliers.

The noise benefits of the tested landing gear and gear cavity technologies were determined from comparisons with baseline G-III data obtained during the ARM-III test. Data from flap deflection angles of 20° and 39° at multiple directivity angles were analyzed. For the 20° flap deflection, the combination of gear fairings plus cavity chevrons and foam produced the quietest configuration, providing overhead noise reductions of 5 dB at frequencies below 400 Hz and 3-4 dB at frequencies above 400 Hz. The removal of chevrons from the cavity (i.e., fairings plus foam installed) resulted in decreased noise reduction only in the 200 Hz < f < 400 Hz range. Surprisingly, good noise reduction was delivered by the combination of cavity chevrons and foam, despite marginal weather conditions that possibly affected the uncertainty at high frequencies. For the 39° flap deflection, lower reductions (on the order of 2 to 3dB) were observed for all tested technology combinations – integration of the MLG region for this configuration contained contributions from inboard flap tip sources that masked the true performance of the gear and cavity technologies. The noise benefits were slightly better at forward directivity angles for both flap deflections, with the combination of gear fairings plus cavity chevrons and foam providing the best performance. In general, the results showed that the tested landing gear fairings and gear cavity treatments are highly effective at mitigating the noise produced by undercarriage systems, even in the presence of conventional (Fowler) flaps.

References

[1] Adib, M., Catalano, F., Hileman, J., Huff, D., Ito, T., Joselzon, A., Khaletskiy, Y., Michel, U., Mongeau, L., and Tester B.J., "Novel Aircraft-Noise Technology Review and Medium- and Long-Term Noise Reduction Goals," International Civil Aviation Organization, Doc. 10017, 2014.

[2] https://www.faa.gov/data_research/aviation/aerospace_forecasts/media/FY2016-36_FAA_Aerospace_Forecast.pdf, accessed October 24, 2016.

[3] Dobrzynski, W., "Almost 40 Years of Airframe Noise Research: What Did We Achieve," *J. Aircraft*, Vol. 47, No. 2, March-April 2010, pp. 353–367.

[4] Khorrami, M. R., Humphreys, W. M. Jr., Lockard, D. P., and Ravetta, P. A., "Aeroacoustic Evaluation of Flap and Landing Gear Reduction Concepts," AIAA Paper 2014-2478, June 2014.

[5] Khorrami, M. R., Lockard, D. P., Humphreys, W. M. Jr., and Ravetta, P. A., "Flight-Test Evaluation of Airframe Noise Mitigation Technologies," AIAA paper 2018-2972, June 2018.

[6] Baumann, E. and Waggoner, E., "Flight and Ground Operations in Support of Airframe Noise Reduction Tests," 2018 AIAA/CEAS Aeroacoustics Conference, AIAA paper 2018-2970, June 2018.

[7] Humphreys, W. M. Jr., Lockard, D. P., Khorrami, M. R., Culliton, W. G., McSwain, R. G., Ravetta, P. A., and Johns, Z., "Development and Calibration of a Field-Deployable Microphone Phased Array for Propulsion and Airframe Noise Flyover Measurements," AIAA Paper 2016-2898, May-June 2016.

[8] Lockard, D. P. and Bestul, K. A., "The Impact of Local Meteorological Conditions on Airframe Noise Flight Test Data," AIAA Paper 2018-2971, June 2018.

[9] AVEC Time Domain Beamforming Software, Ver. 2.85, AVEC, Inc., Blacksburg, VA, URL: http://www.avec-engineering.com/products.html, cited March 21, 2019.

[10] Guo, Y., "Aircraft Flap Side Edge Noise Modeling and Prediction," AIAA Paper 2011-2711, June 2011.

[11] Rossignol, K. S., "Development of an Empirical Prediction Model for Flap Side-Edge Noise," AIAA Paper 2010-3836, June 2010.

[12] Rossignol, K. S., "Flow Field Measurements to Characterize Flap Side-Edge Noise Generation," AIAA Paper 2013-2061, May 2013.

[13] Khorrami, M. R., Humphreys, W. M. Jr., and Lockard, D. P., "An Assessment of Flap and Main Landing Gear Noise Abatement Concepts," AIAA paper 2015-2987, June 2015.

[14] Ravetta, P. A., Wisda, D. M., Khorrami, M. R., and Van de Ven, T., "Assessment of Airframe Noise Reduction Technologies based on EPNL from Flight Tests," Paper to be presented at the 25th AIAA/CEAS Aeroacoustics Conference in Delft, The Netherlands, May 2018.